

Numerical model of self-propulsion in a fluid

D.J.J Farnell, T David and D.C Barton

J. R. Soc. Interface 2005 **2**, 79-88
doi: 10.1098/rsif.2005.0027

References

This article cites 31 articles, 13 of which can be accessed free
<http://rsif.royalsocietypublishing.org/content/2/2/79.full.html#ref-list-1>

Email alerting service

Receive free email alerts when new articles cite this article - sign up in the box at the top right-hand corner of the article or click [here](#)

To subscribe to *J. R. Soc. Interface* go to: <http://rsif.royalsocietypublishing.org/subscriptions>

Numerical model of self-propulsion in a fluid

D. J. J. Farnell^{1,†}, T. David² and D. C. Barton³

¹Unit of Ophthalmology, School of Clinical Science, Department of Medicine, Daulby Street, University of Liverpool, Liverpool L69 3GA, UK

²Department of Mechanical Engineering, University of Canterbury, Private Bag 4800, Christchurch, New Zealand

³School of Mechanical Engineering, University of Leeds, Woodhouse Lane, Leeds LS2 9JT, UK

We provide initial evidence that a structure formed from an articulated series of linked elements, where each element has a given stiffness, damping and driving term with respect to its neighbours, may ‘swim’ through a fluid under certain conditions. We derive a Lagrangian for this system and, in particular, we note that we allow the leading edge to move along the x -axis. We assume that no lateral displacement of the leading edge of the structure is possible, although head ‘yaw’ is allowed. The fluid is simulated using a computational fluid dynamics technique, and we are able to determine and solve Euler–Lagrange equations for the structure. These two calculations are solved simultaneously by using a weakly coupled solver. We illustrate our method by showing that we are able to induce both forward and backward swimming. A discussion of the relevance of these simulations to a slowly swimming body, such as a mechanical device or a fish, is given.

Keywords: numerical; simulation; self-propulsion; fluid; structure

1. INTRODUCTION

In this article, we wish to show by using a numerical approach that a simple articulated structure may propel itself through a fluid, and we provide preliminary investigations to illustrate our method. We shall assume that the fluid may be viewed as two-dimensional (2D) continuum (such as in a soap film) and that our structure has no depth, and so may be assumed to be one-dimensional (1D). We restrict our simulations to those cases in which the motion of the mechanical structure lies in the 2D plane. Another explicit assumption of the calculations is that the head of the structure always lies on the x -axis and points in the direction of motion. We wish to present the method in this article and illustrate this approach by looking at cases that have relatively low Reynolds number (Re) of approximately 250. We note that this choice for Re aids numerical stability, and we intend to consider the more challenging situation of higher Re in future calculations.

Experiments concerning the properties of soap films have recently been carried out (Martin & Wu 1995; Chomaz & Cathalau 1996; Rutgers *et al.* 1996; Zang *et al.* 2000), and these systems have been proposed as the experimental versions of theoretical 2D liquids. Indeed, we note that particularly interesting fluidic properties were observed when a silk filament was introduced into the flowing soap film (Zang *et al.* 2000). Such flapping filaments or flags have been pointed out to have a clear relevance to swimming fishes (Huber 2000).

We note that problems that are conceptually similar to the problem of our ‘swimming structure’ have previously been treated with considerable success by using a so-called ‘weakly coupled’ solver. We shall adopt this approach here, and examples of such problems are a single filament (Farnell *et al.* 2004a) and coupled filaments in a flowing soap film (Farnell *et al.* 2004b), and the motion of the leaflets in artificial heart valves (Horsten 1990; Fenlon & David 2001a, b; Farnell *et al.* 2004c). Our approach has therefore been extensively tested for these systems; thus, we shall not extensively test the methodology again here, and the interested reader is referred to these references for more information. Furthermore, the validity and accuracy of our approach has also been proven in these extensive earlier calculations. We now wish to extend the range of applicability of our approach and hope only to show that, in theory, a simple articulated structure is able to propel itself through a fluid.

We note that two main methods have been used in the past to investigate theoretically the motion of elongated animals in fluids. Taylor’s theory (Taylor 1952) was based essentially on a resistive model, whereas that of Lighthill (1960) used a ‘reactive’ analysis, where the investigation concentrated on the reactive forces between a small volume of fluid and the animal’s surface in contact with the fluid. However, a review by Lighthill (1969) showed that the resistive method seemed to provide the best results for elongated vertebrae. The swimming action of fishes has also been studied both experimentally (Gray 1933, 1955; D’Août & Aerts 1997, 1999; Drucker & Lauder 1999; Sfaliotakis *et al.* 1999)

[†]Author for correspondence (d.farnell@liverpool.ac.uk).

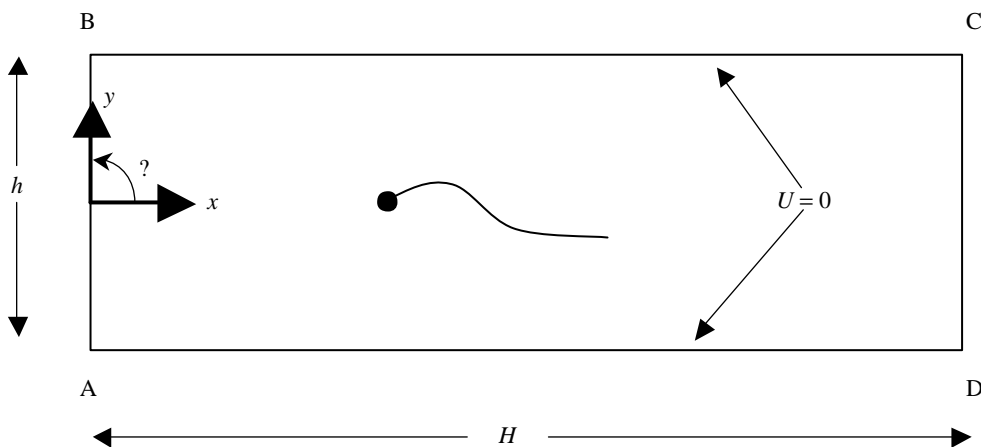


Figure 1. The computational fluid domain. Note that non-slip boundary conditions are imposed on the fluid mesh edges AD and BC, and that the motion of the mechanical structure is imposed on the fluid as a moving boundary condition. Stress-free boundary conditions are imposed at both the inlet AB and the outlet CD.

and theoretically (Gray & Hancock 1955; Williams *et al.* 1995; Liu *et al.* 1996; Sigvardt & Williams 1996; Carling *et al.* 1998; Liu & Kawachi 1999; Long *et al.* 2002; Huber 2000).

We begin our treatment of this system by firstly considering our mathematical and numerical methodology in detail. We then illustrate our methodology by presenting results for our initial studies of this system, and show that we may induce either backward or forward motion by simply changing the form of the driving terms acting along the length of the mechanical structure. We then discuss the relevance of our studies to swimming action of fishes and/or mechanical devices (Sfaiiotakis *et al.* 1999). We conclude by summarizing our results and considering other possible future applications.

2. METHOD

2.1. The Navier–Stokes equations

We assume that the fluid is incompressible, with a viscosity that is Newtonian in form, and that the density is constant. In addition, we use similar assumptions to those used in experiments for measuring the viscosity of soap films (Martin & Wu 1995). The flow is treated as being isothermal and laminar, and an argument for this assumption is given below. The relevant time-dependent equations are thus given by the Navier–Stokes equations,

$$\frac{D\tilde{\vec{u}}}{Dt} = -\frac{1}{\rho}\nabla\tilde{p} + \nu\nabla^2\tilde{\vec{u}}, \quad (2.1a)$$

$$\nabla \cdot \tilde{\vec{u}} = 0. \quad (2.1b)$$

Here, $\tilde{\vec{u}} = \{\tilde{u}, \tilde{v}\}$ is the 2D vector field corresponding to the x - and y -directions as shown in figure 1, \tilde{p} is the fluid pressure, ρ is the density of the fluid and ν is the kinematic viscosity of the fluid. We non-dimensionalize the fluid equations such that

$$\begin{aligned} x &= \frac{\tilde{x}}{L}, & y &= \frac{\tilde{y}}{L}, & u &= \frac{\tilde{u}}{U}, & v &= \frac{\tilde{v}}{U}, \\ t &= \frac{\tilde{t}U}{L}, & p &= \frac{\tilde{p}}{\rho U^2}, \end{aligned} \quad (2.2)$$

where L is the actual (dimensional) length of the mechanical structure and U is a (dimensional) characteristic speed (e.g. the swimming speed of the mechanical structure). Equation (2.1a,b) now becomes

$$\frac{D\tilde{\vec{u}}}{Dt} = -\nabla p + Re^{-1}\nabla^2\tilde{\vec{u}}, \quad (2.3a)$$

$$\nabla \cdot \tilde{\vec{u}} = 0, \quad (2.3b)$$

where the Re is given by $Re = LU/\nu$. We assume the fluid domain is as given in figure 1; namely, a channel with an inlet and outlet. Non-slip boundary conditions are assumed on the walls of the channel, and ‘natural’ (or stress-free) boundary conditions are assumed at the inlet and outlet. We note that the width h of the channel is also set to one (non-dimensional) unit. The width of the mechanical structure is assumed to be 0.04 non-dimensional units and we set the Re to be $Re=250$, as this aids numerical stability (see §4). The length H of the channel is 15 (non-dimensional) units, far enough away from the mechanical structure so that the outlet boundary has negligible effect. The mechanical structure is placed initially approximately at the mid-point of the channel. Details (see also Fenlon *et al.* 2001; Farnell *et al.* 2004a,b) of performing a computational fluid dynamics (CFD) calculation are presented in §5. A fuller investigation of the effects of varying the values for these parameters on our calculations will be considered in a future article.

3. THE EULER–LAGRANGE EQUATIONS

Similar to earlier calculations (Williams *et al.* 1995, Sigvardt & Williams 1996; Carling *et al.* 1998), we

assume that the mechanical structure is composed of N equal length, homogeneous, rigid elements. The (dimensional) length of each element is \tilde{l} and the (dimensional) mass of each element is \tilde{m} . However, in our case, the elements are fixed to one another at their hinge (or fulcrum) points, and the mechanical structure is thus assumed to be approximated by a form of N -tuple pendulum, in which each hinge has a positive spring stiffness coefficient and a positive damping coefficient associated with it. We assume that no lateral displacement of the head in the y -direction may occur where this assumption is supported by experiment (Gray 1933, 1955). However, head yaw is allowed, as the angle that the first element makes with the x -axis does not have to be zero. We note that the leading edge of the mechanical structure is allowed to move in the x -direction only. Each element s makes an angle θ_s with the horizontal x -axis and the position of the leading edge of the mechanical structure on the x -axis is given by \tilde{x}_0 . In analogy with previous studies (Farnell *et al.* 2004a–c), the Langrangian Ψ may be shown to be given by

$$\begin{aligned} \Psi = & \frac{1}{2} \tilde{m} \tilde{l}^2 \sum_{i=1}^N \sum_{j=1}^{i-1} \sum_{k=1}^{i-1} \dot{\theta}_j \dot{\theta}_k \cos(\theta_j - \theta_k) \\ & + \frac{1}{2} \tilde{m} \tilde{l}^2 \sum_{i=1}^N \dot{\theta}_i \sum_{j=1}^{i-1} \dot{\theta}_j \cos(\theta_i - \theta_j) \\ & + \frac{1}{6} \tilde{m} \tilde{l}^2 \sum_{i=1}^N \dot{\theta}_i^2 - \dot{\tilde{x}}_0 \tilde{m} \tilde{l} \sum_{i=1}^N \sum_{j=1}^{i-1} \dot{\theta}_j \sin(\theta_j) \\ & - \frac{1}{2} \dot{\tilde{x}}_0 \tilde{m} \tilde{l} \sum_{i=1}^N \dot{\theta}_i \sin(\theta_i) + \frac{1}{2} \dot{\tilde{x}}_0^2 \tilde{m} N \\ & - \frac{1}{2} \sum_{i=1}^N \tilde{K}_i (\theta_i - \theta_{i-1})^2, \end{aligned} \quad (3.1)$$

where the terms due to the stiffness \tilde{K}_s at each hinge are valid only for small values of $\theta_s - \theta_{s-1}$, $\forall s$ (and that $\theta_0 = \dot{\theta}_0 = 0$). Note that the subscript s for the element angles runs from 1 to N , although we may define—notationally only—an angle θ_0 , which aids our definition of the potential energy in equation (3.1). (However, we do assume that the minimum potential energy position is given by a profile in which the angle for the leading edge element is zero.)

The Langrangian given by equation (3.1) may now be used to obtain the Euler–Lagrange equations by writing

$$\frac{d}{dt} \left(\frac{\partial \Psi}{\partial \dot{\theta}_s} \right) - \frac{\partial \Psi}{\partial \theta_s} = \tilde{f}_s \quad \forall s, \quad \frac{d}{dt} \left(\frac{\partial \Psi}{\partial \dot{\tilde{x}}_0} \right) - \frac{\partial \Psi}{\partial \tilde{x}_0} = \tilde{g}, \quad (3.2)$$

where \tilde{f}_s and \tilde{g} represent non-conservative external torques and forces, respectively. The function \tilde{f}_s represents the externally applied torques exerted on a given element s , and these torques are non-conservative. We subdivide the terms within this function into

two distinct pieces, given by

$$\begin{aligned} \tilde{f}_s = & -\tilde{C}_s(\dot{\theta}_s - \dot{\theta}_{s-1}) - \tilde{C}_{s+1}(\dot{\theta}_s - \dot{\theta}_{s+1}) \\ & + \frac{1}{2} \tilde{\Delta}_s \tilde{l} + \tilde{Q}_s(\tilde{t}). \end{aligned} \quad (3.3)$$

We note that $\tilde{Q}_s(\tilde{t})$ contains the driving-term to our equations and corresponds to the ability of the mechanical structure to cause torques along its length (see §4 for more details). The damping terms are thus encoded in the terms $\tilde{C}_s(\dot{\theta}_s - \dot{\theta}_{s-1}) + \tilde{C}_{s+1}(\dot{\theta}_s - \dot{\theta}_{s+1})$, and favour a difference between angular velocities of successive elements (both above and below a particular element s) that is small. An inflexible system is thus approximated by having large values for both \tilde{K}_s and \tilde{C}_s . The term $\tilde{\Delta}_s$ in equation (3.3) refers to external pressure forces (as distinct from the internal stiffness and damping terms or, indeed, the driving terms) acting on the mechanical structure elements creating a torque of strength $1/2\tilde{\Delta}_s\tilde{l}$, which in this case are caused by the fluid pressures forces generated by the liquid. For the present case, we can show from an order of magnitude argument that the pressure forces are much larger than those exerted by viscosity and hence the viscous shear forces acting parallel to the N -tuple pendulum are considered negligible.

We also note that the non-conservative forces for the leading edge generalized variable \tilde{x}_0 are given by

$$\tilde{g} = - \sum_{i=1}^N \tilde{\Delta}_i \sin(\theta_i). \quad (3.4)$$

We solve these equations using adaptive step-sized Runge–Kutta method (see Farnell *et al.* 2004a–c for more details). Equation (2.3a,b) is solved using a commercial code (FIDAP). Although our solutions are mesh independent, we do not fully investigate the variation of our solution with respect to the width of mechanical structure and Re . We wish to present only the initial calculations and thereby investigate whether our new approach might be used to give reasonable results. We now non-dimensionalize the Euler–Lagrange equations by introducing (as before) characteristic scales for mass, length, velocity and time, such that

$$m = \frac{\tilde{m}}{M}, \quad l = \frac{\tilde{l}}{L}, \quad t = \frac{\tilde{t}U}{L}. \quad (3.5)$$

The quantities \tilde{K}_s , \tilde{C}_s and $\tilde{\Delta}_s$ may also be non-dimensionalized in a similar manner to give

$$K_s = \frac{\tilde{K}_s}{U^2 M}, \quad C_s = \frac{\tilde{C}_s}{UML}, \quad \Delta_s = \frac{\tilde{\Delta}_s L}{MU^2}. \quad (3.6)$$

The non-dimensionalized Euler–Lagrange equations for the element angles are given by

$$\begin{aligned}
& \sum_{i=1}^{s-1} \ddot{\theta}_i \cos(\theta_s - \theta_i) \left(N - s + \frac{1}{2} \right) \\
& + \sum_{i=s}^N \ddot{\theta}_i \cos(\theta_s - \theta_i) \left(N - i + \frac{1}{2} \right) \\
& - \frac{1}{6} \ddot{\theta}_s + \sum_{i=1}^{s-1} \dot{\theta}_i^2 \sin(\theta_s - \theta_i) \left(N - s + \frac{1}{2} \right) \\
& + \sum_{i=s}^N \dot{\theta}_i^2 \sin(\theta_s - \theta_i) \left(N - i + \frac{1}{2} \right) \\
& + \frac{K_s}{ml^2} (\theta_s - \theta_{s-1}) + \frac{K_{s+1}}{ml^2} (\theta_s - \theta_{s+1}) \\
& + \frac{C_s}{ml^2} (\dot{\theta}_s - \dot{\theta}_{s-1}) + \frac{C_{s+1}}{ml^2} (\dot{\theta}_s - \dot{\theta}_{s+1}) \\
& - \frac{1}{l} \ddot{x}_0 \left(N - s + \frac{1}{2} \right) \sin(\theta_s) \\
& = \frac{\Delta_s}{2ml} + \frac{\mathcal{Q}_s(t)}{ml^2}, \tag{3.7}
\end{aligned}$$

and the non-dimensionalized Euler–Lagrange equation for the leading-edge term is given by

$$\begin{aligned}
& \frac{N}{l^2} \ddot{x}_0 - \frac{1}{l} \sum_{i=1}^N \left(N - i + \frac{1}{2} \right) \ddot{\theta}_i \sin(\theta_i) \\
& - \frac{1}{l} \sum_{i=1}^N \left(N - i + \frac{1}{2} \right) \dot{\theta}_i^2 \cos(\theta_i) \\
& = -\frac{1}{ml^2} \sum_{i=1}^N \Delta_i \sin(\theta_i). \tag{3.8}
\end{aligned}$$

The pressure force acting on an element of the mechanical structure in the dimensional system in our Euler–Lagrange equations (namely $\tilde{\Delta}_s$) must be related to the pressure difference (between those pressures acting on the bottom, $\tilde{p}_s^{\text{bottom}}$, and the top, \tilde{p}_s^{top} , of a mechanical structure element) such that

$$\delta \tilde{p}_s = \tilde{p}_s^{\text{bottom}} - \tilde{p}_s^{\text{top}} \Rightarrow \tilde{\Delta}_s = \tilde{l} \delta \tilde{p}_s. \tag{3.9}$$

The non-dimensional form of this equation is given by

$$\Delta_s = \left(\frac{\rho_f L^2}{M} \right) l \delta p_s = F l \delta p_s, \tag{3.10}$$

where ρ_f is the 2D density of the fluid. Furthermore, we note that we may express the mass of the mechanical structure in the experimental (dimensional) system in terms of a *linear density*, σ , such that $F = \rho_f L / \sigma$. Again, note that we assume that our idealized mechanical structure is 1D.

4. VALUES FOR THE PARAMETERS

We choose values for the parameters such that they are consistent with earlier simulations for different, although related, systems (Fenlon & David 2001a,b; Farnell *et al.* 2004a–c). In particular, we choose a value for F of unity. As we wish to prove the principle of whether we are able to simulate any of the observed properties of the system, we feel that this is a reasonable assumption. In a similar manner, we set the Re to be

$Re=250$ as this aids numerical stability. Note that inertial forces are dominant and viscous forces are usually neglected for $10^3 < Re < 10^5$ (Sfaliotakis *et al.* 1999).

The fluid is initially at rest and non-slip boundary conditions are imposed on the walls of the channel, while the inlet and outlet have stress-free boundary conditions. We choose a fluid mesh such that there are at least four mesh nodes within the width of the mechanical structure. All of the parameters above are chosen to be in reasonable agreement with those experimental values given elsewhere (D'Août & Aerts 1997, 1999; Drucker & Lauder 1999; Sfaliotakis *et al.* 1999).

The values for the stiffness, damping and driving terms are chosen to induce either forward or backward swimming. For the case of the backward swimming mode, we keep the stiffness and damping terms constant, where

$$K_s = 0.75, \quad C_s = 0.01 \quad \forall s = \{1, \dots, N\}, \tag{4.1}$$

and we set the driving terms to have a travelling wave form, given by

$$\mathcal{Q}_s(t) = A \sin\left(2\pi\omega t + \frac{2\pi\lambda(s-1)}{N}\right). \tag{4.2}$$

In this case, $A=0.03$ and $\omega=1.0$. The stiffness and damping terms for the forward swimming mode are set to be constant but of greater magnitude (to reduce head yaw), where

$$K_s = 5.0, \quad C_s = 0.1 \quad \forall s = \{1, \dots, N\}. \tag{4.3}$$

The driving terms for the forward swimming mode are given by

$$\mathcal{Q}_s(t) = \frac{A(s-1)}{N} \sin\left(2\pi\omega t + \frac{2\pi\lambda(s-1)}{N}\right), \tag{4.4}$$

with $A=0.2$ and $\omega=1.0$. We see from equation (4.4) that the driving terms of the mechanical structure are much stronger at the tail than at the head for the forward swimming mode. Our calculations were tested for